RSC Advances

A molecular cobalt catalyst supported by an amine-bis(phenolate) ligand for both electrolytic and photolytic water reduction

Journal:	*RSC Advances*
Manuscript ID	RA-ART-07-2015-014753.R1
Article Type:	Paper
Date Submitted by the Author:	23-Sep-2015
Complete List of Authors:	Zhan, Shuzhong; College of Chemistry ? Chemical Engineering, South China University of Technolog, ; Fu, Ling-Zhi; South China University of Technology, Zhou, Ling-Ling; South China University of Technology,
Subject area & keyword:	

Journal Name

RSCPublishing

ARTICLE

A molecular cobalt catalyst supported by an amine-bis(phenolate) ligand for both electrolytic and photolytic water reduction

Cite this: DOI: 10.1039/x0xx00000x

Received 00th January 2012,
Accepted 00th January 2012

DOI: 10.1039/x0xx00000x

www.rsc.org/

Ling-Zhi Fu, Ling-Ling Zhou and Shu-Zhong Zhan*

A new molecular catalyst based on cobalt complex $[L_2Co_2Cl_2]$ **1** is prepared by the reaction of an amine-bis(phenolate) ligand (H_2L) with $CoCl_2 \cdot 6H_2O$ for both electrolytic and photolytic water reduction. **1** can electrocatalyze hydrogen evolution from water with a turnover frequency (TOF) of 789.6 moles of hydrogen per mole of catalyst per hour at an overpotential of 837.6 mV (pH 7.0). **1** in pH 6.0 aqueous solution under air, together with $[Ru(bpy)_3]Cl_2$ and ascorbic acid, in the presence of blue light (λ_{max} = 469 nm) also produces hydrogen with a turnover number (TON) = 912 mol of H_2 (mol of cat)$^{-1}$.

Introduction

Hydrogen, when generated directly from water, is a promising chemical fuel for sustainable energy supplies. [1-3] In particular, electro- and photo-catalytic methods for generating hydrogen from water have been explored as cost-effective ways of producing a carbon-neutral fuel. Currently, one of the key challenges to water splitting is the development of efficient catalysts for the water reduction reactions with high turnover rates, low overpotentials, and good stability. [4,5] Electrocatalytic H_2 evolution has been reported for a variety of earth abundant transition metal complexes in aqueous media.[6-12] However, the development of photocatalytic systems intended to drive hydrogen evolution from water using visible light still remains a challenging subject. [13,14] Many research groups, including ours, have focused on the design of molecular photo-catalysts for the reduction of water to form H_2. [15-23] Among these, cobalt complexes supported by tetra- and pentadentate ligands have been reported for the catalytic production of H_2 in aqueous solution. [24-27] Webster and co-workers used a neutral pentadentate ligand, N,N-bis(2-pyridinylmethyl)-2,2'-bipyridine-6-methanamine (DPA-Bpy) to assembly a molecular cobalt catalyst, $Co(DPA\text{-}Bpy)Cl_2$ for both electrocatalytic and photocatalytic water reductions. [28] It has been shown that the donor type and electronic properties of the ligands play vital roles in determining the structure and reactivity of the corresponding metal complexes. [29-32] Identification of the factors that control the oxidation/reduction site in these complexes, determining of their redox potentials and characterization of their electronic structures, is critical for the design of more effective molecular catalysts for H_2 production. With this mind, we have been studying tetradentate ligands such as amine-bis(phenolate) ligands and their corresponding cobalt complexes, and especially their

catalytic properties. [33,34] In this paper, we present the synthesis and characterization of one new cobalt(III) complex $[L_2Co_2Cl_2]$, as well as its electro- and photo-catalytic properties for water reduction.

Results and discussion

In the presence of trimethylamine, the reaction of $CoCl_2 \cdot 6H_2O$ and H_2L provides a dinuclear cobalt (III) complex **1** (yield = 56 %) (Scheme 1). The UV/Vis spectrum of **1** in MeCN shows a absorption peak at 263 nm (Fig. S1), which can be assigned to that of ligand. To investigate the stability of complex **1,** UV/Vis spectra of **1** were measured in buffered aqueous solutions at the pH range 2.8 -10.5. As shown in Figs. S2-S3, the intensity of the absorption band at 263 nm slightly increased (from pH 2.8 to 10.5), but the peak position did not change, indicating this complex is stable under these conditions.

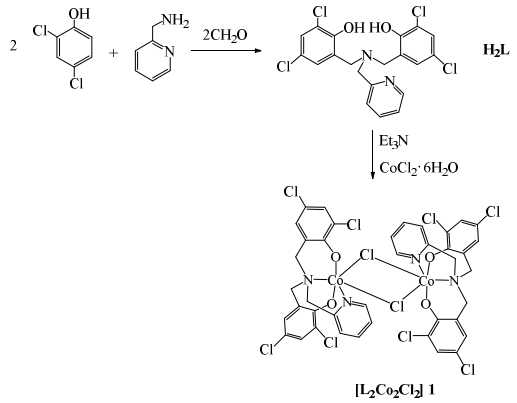

Scheme 1. Schematic representation of the synthesis of $[L_2Co_2Cl_2]$ **1**

Complex **1** crystallizes in space group P_1_21/c_1, with two units present per unit cell. As shown in Fig. 1, the molecular structure of **1** is formed by two L^{2-} ligands, two cobalt ions and two Cl^- ions. The observed Co-N bond distances are 1.905(4) and 1.972(4) Å, respectively and the bond distances of Co-O fall in the range 1.906(4) to 1.913(4) Å. Two cobalt ions are linked by two Cl^- ions, and the distance between two cobalt atoms is 2.9084(14) Å. The Co(1)−Cl(1)−Co(1)# angle in **1** was 98.98(17)°, and the chlorides are orientated *cis* to the nitrogen on the pendant pyridyl group. The Co−Cl bond distances are 1.909(4) and 1.916(4) Å, respectively. The distance between two cobalt atoms is 2.9084(14) Å.

From Fig. 2a, the cyclic voltammogram of 0.25 mM complex **1** in DMF shows one reversible Co^{III}/Co^{II} redox couple at $E_{1/2}$ = -0.80 V and one quasi-reversible Co^{II}/Co^{I} redox couple at -1.58 V, respectively. The current response of the redox event at -1.58 V shows linear dependence on the square root of the scan rate (Fig. S4), which is an indicative of a diffusion-controlled process, with the electrochemically active species freely diffusing in the solution.

To determine possible electrocatalytic activity of this complex, cyclic voltammograms of complex **1** were recorded in the presence of acetic acid. From Fig. 2b it can be seen that the current near -0.90 and -1.64 V increased markedly with increasing proton concentration (acetic acid concentration increased from 0.00 to 3.40 mM). This rise in current can be attributed to the catalytic generation of H_2 from acetic acid. [35] The result indicates that hydrogen evolution electrocatalyzed by **1** requires the reduction of Co(III) to Co(II) or Co(II) to Co(I) and protonation. Interestingly, with the acetic acid concentration increased from 0.0 to 3.40 mM (Fig. 2b), the onset of the catalytic waves move to higher potentials from -0.64 to -0.36 V versus $Ag/AgNO_3$. Based on the above observations, both couples Co^{III}/Co^{II} and Co^{II}/Co^{I} are devoted to proton reduction, which is different from previous reports that only couple Co^{II}/Co^{I} is devoted to proton reduction. [36,37] Further mechanistic studies are under investigation.

A number of control experiments were carried out to verify that complex **1** is responsible for the catalysis. In particular, the free ligand, $CoCl_2 \cdot 6H_2O$, and the mixture of the free ligand and $CoCl_2 \cdot 6H_2O$ were each measured under identical conditions. As can be seen in Fig. S5-Fig. S7, the catalytic competency achieved with **1**

is not matched by just ligand, $CoCl_2 \cdot 6H_2O$, or the mixture of the free ligand and $CoCl_2 \cdot 6H_2O$, as might arise from dissociation of the ligand, nor can it be accomplished with the ligand bound to a redox-inactive metal. Thus, a combination of the cobalt center and the ligand is essential for catalytic activity.

Further evidence for the electro-catalytic activity was obtained by bulk electrolysis of a DMF solution of complex **1** (2.5 μM) with acetic acid (5.0 mM) at variable applied potential using a glassy carbon plate electrode in a double-compartment cell. Fig. 3a shows the total charge of bulk electrolysis of complex **1** in the presence of acid, the charge significantly increased when the applied potentials was set to more negative. When the applied potential was -1.45 V versus $Ag/AgNO_3$, the maximum charge reached 14 mC during 2 min of electrolysis, accompanying evolution of a gas, which was confirmed as H_2 by gas chromatography. According to Fig. S8, ~1.70 μL of H_2 was produced over an electrolysis period of 2 h. A controlled-potential electrolysis (CPE) experiment under the same potential with a catalyst-free solution only gave a charge of 3 mC (Fig. 3b), showing that this complex does serve an effective hydrogen production under such conditions. Assuming every catalyst molecule was distributed on the electrode surface and every electron was used for the reduction of protons, according to *eq*. (1), [33] we calculated TOF for the catalyst reaching a maximum of 20.79 moles of hydrogen per mole of catalyst per hour at an overpotential of 941.6 mV (Eq. S1 and Fig. S9).

$$TOF = \Delta C / (F * n_1 * n_2 * t) \qquad (1)$$

Where, ΔC is the charge from the pre-catalyst solution during CPE minus the charge from solution without pre-catalyst during CPE; F is Faraday's constant, n_1 is the number of moles of electrons required to generate one mole of H_2, n_2 is the number of moles of pre-catalyst in solution, and t is the duration of electrolysis.

To study the electrochemical behavior of complex **1** in water, CVs were conducted in buffered aqueous solutions where pH = 2.8−7.0, which is the range associated with catalytic water reduction. In a pH 7.0 solution, an irreversible Co^{III}/Co^{II} wave was observed at –0.32 V versus Ag/AgCl (Fig. 4-inset). To probe the nature of this reduction process, we investigated the pH dependence of the cathodic peak potential. The reduction waves were shifted to higher potentials under lower pHs, which reflects the shifts in the thermodynamic potential for electrocatalysis (Fig. 4). Scanning to cathodic potentials beyond the first irreversible reduction revealed another irreversible redox event at a cathodic peak potential of $E_{p,c}$ = -1.73 V versus Ag/AgCl, which is assigned to the couple of Co^{II}/Co^{I} and dependent of pH (Fig. 4), indicating this electron-transfer is devoted to water reduction. Interestingly, with the pHs decreased from 7.0 to 2.8, the onset of the catalytic waves were shifted to higher potentials from -1.40 to -1.0 V versus Ag/AgCl (Fig. 4). As shown in Fig. 5a, in the absence of complex **1**, a catalytic current was not apparent until a potential of -1.52 V versus Ag/AgCl was attained. With addition of complex **1** (120.6 μM), the onset of catalytic current was observed at about -1.20 V versus Ag/AgCl, and the current strength increased significantly with increasing concentrations of complex **1** from 0.00 to 120.6 μM (Fig. 5a).

Further evidence for the electro-catalytic activity was also obtained by bulk electrolysis of a 2.0 μM complex **1** in 0.25 M buffer at variable applied potentials. When the applied potential was -1.45 V versus Ag/AgCl, the maximum charge was only 16 mC during 2 min of electrolysis in absence of complex **1** (Fig. 5b). Under the same conditions, the charge reached 446 mC with addition of complex **1** (Fig. 5c), accompanying a large amount of gas bubble appeared, which was confirmed to be H_2 by GC analysis. The evolved H_2 was analyzed by gas chromatography, Fig. S10a, which gave 3.38 mL of H_2 over an electrolysis period of 1 h with a Faradaic

efficiency of 92.08% for H_2 (Fig. S10b). TOF for electrocatalytic hydrogen production by complex **1** is 789.6 moles of hydrogen per mole of catalyst per hour at an overpotential of 837.6 mV (pH 7.0) (Eq. S2 and Fig. S11).

To prove complex **1** as a homogeneous electrocatalyst, we obtained dependence of the catalytic current on complex **1** concentration. As shown in Fig. 5a, the observation of the catalytic current being dependent of the complex concentration could indicate a homogeneous catalyst. And several pieces of evidence also suggest that this cobalt complex is a homogeneous catalyst: 1) There is no evidence for a heterogeneous electrocatalytic deposit. For example, the electrode was rinsed with water and electrolysis at -1.45 V vs Ag/AgCl was run for an additional 2 min in a 0.25 M phosphate buffer at pH 7.0 with no catalyst present in solution. During this period, ca. 16 mC of charge was passed, a similar magnitude as is observed for electrolysis conducted with freshly polished electrode. 2) No discoloration of the electrodes was observed during cyclic voltammetry or bulk electrolysis. 3) Under the same conditions, at a glassy carbon electrode, there was no evidence for precipitation formation by EDS (Fig. S12) after a 3 h electrolysis period.

In order to determine whether **1** retains activity over longer time periods, a 72 h CPE at -1.45 V vs Ag/AgCl was conducted in a stirred 0.25 M buffer solution (pH 7.0), containing **1** (4.5 μM). As shown in Fig. S13a, a total of 1400 C was passed during the electrolysis. This catalyst afforded a charge build-up over time, with no substantial loss in activity over the course of 72 h. After a 72 h electrolysis period, pH increases by 5 units (from 7.0 to 12), consistent with accumulation of OH^- by water reduction, $2H_2O + 2e \rightarrow H_2 + 2OH^-$. Fig. S13b shows that the catalytic current is sustained for at least 72 h**.**

We also explored photocatalytic water reduction by complex **1** using ascorbic acid as electron donor and $[Ru(bpy)_3]Cl_2$ as photosensitizer. The capability of **1** to foster hydrogen evolution in light activated experiments was tested upon continuous visible irradiation (LED lamp, λ = 469 nm) of 0.25 M buffer solutions containing different concentrations of **1** in the presence of $Ru(bpy)_3Cl_2$ as photosensitizer and ascorbic acid as sacrificial electron donor.

The influence of the pH on the activity of H_2 evolution by complex **1** was investigated in the pH range of 3−7. As shown in Fig. S14, the best pH for photocatalytic H_2 evolution by complex **1** (0.10 mM) was observed at pH 6.0, a more closer to neutral media, with a TON of 965 mol of H_2 (mol of cat)$^{-1}$. This is different from the reported results that the best pH for photocatalytic H_2 evolution by photo-catalyst was observed at pH 4.0. [28,38] The light-induced H_2 generation catalyzed by **1** depends on the concentrations of sacrificial reagent and photosensitizer. For the photocatalytic systems containing 0.15 M ascorbic acid, 0.10 mM complex **1** and varying $Ru(bpy)_3Cl_2$, the TON used in 2 h increases with increasing the concentrations of $Ru(bpy)_3Cl_2$ until a saturation value of 486 mol of H_2 (mol of cat)$^{-1}$ is reached at 0.90 mM. Then, the TON decreased when the concentrations of $Ru(bpy)_3Cl_2$ was set to more (Fig. S15).

For the photocatalytic systems containing 0.70 mM $Ru(bpy)_3Cl_2$, 0.10 mM complex **1** and varying ascorbic acid, the TON used in 2 h increases with increasing the concentrations of ascorbic acid (Fig. S16). To investigate the concentration effect on H_2 production, we carried out photolysis at different concentrations of **1** ranging from 0.02 to 0.10 mM at pH 6.0. As shown in Fig. 6, **1**

catalyzes H_2 production with a TON of 456 mol of H_2 (mol of cat)$^{-1}$ at 0.10 mM **1** (under air). When the concentration of **1** was lowered to 0.02 mM, the TON increased significantly to 912 mol of H_2 (mol of cat)$^{-1}$ (under air), suggesting that the concentration of **1** has a significant effect on the photocatalytic activity for H_2 production (Fig. S17).

Furthermore, we carried out photolysis under air and Ar, respectively. The amount of H_2 (0.115 mM) produced in the presence of air during the first three hours of irradiation is 63% of that produced when the H_2 evolution was conducted in Ar (0.183 mM), suggesting that O_2 can inhibit the evolution of H_2 (Fig. S18). To identify factors responsible for the photocatalytic H_2 evolution in the above system, we added one of the three components (ascorbic acid, $[Ru(bpy)_3]Cl_2$, or complex **1**) or $CoCl_2{\cdot}6H_2O$ to a reaction flask after cessation of the H_2 evolution to see if the H_2 production could be resumed. However, addition of any of the four components, in the same amount as used in the photocatalytic reaction, resulted in no significant amount of H_2 generation. Both complex **1** and $[Ru(bpy)_3]Cl_2$ need to be added to resume the production of 22 μmol H_2 (Fig. S19). The addition of both ascorbic acid and $[Ru(bpy)_3]Cl_2$ led to an slight increase in H_2 evolution (30 μmol). However, no significant amount of H_2 was produced when both ascorbic acid and $[Ru(bpy)_3]Cl_2$ were added, suggesting the decomposition of both **1** and $[Ru(bpy)_3]^{2+}$ during photolysis.

Experimental

Materials and physical measurements: 2-pyridylamino-N,N-bis(2-methylene-4,6-dichlorophenol) (H_2L) was prepared using literature procedure by employing a Mannich condensation. [39] Elemental analyses for C, H, and N were obtained on a Perkin-Elmer analyzer model 240. IR spectrum was obtained as KBr pellet on a Bruker 1600 FT-IR spectrometer from 4000 to 400 cm^{-1}. UV-Vis spectra were measured on a Hitachi U-3010 spectrometer. Cyclic voltammograms were obtained on a CHI-660E electrochemical analyzer under N_2 using a three-electrode cell in which a glassy carbon electrode (1 mm in diameter) was the working electrode, a saturated $Ag/AgNO_3$ or Ag/AgCl electrode was the reference electrode, and a platinum wire was the auxiliary electrode. In organic media, the ferrocene/ferrocenium (1+) couple was used as an internal standard, and 0.10 M $[(n\text{-}Bu)_4N]ClO_4$ was used as the supporting electrolyte. Controlled-potential electrolysis (CPE) in aqueous media was conducted using an air-tight glass double compartment cell separated by a glass frit. The working compartment was fitted with a glassy carbon plate and an Ag/AgCl reference electrode. The auxiliary compartment was fitted with a Pt gauze electrode. The working compartment contained a 50 mL of 0.25 M phosphate buffer solution, while the auxiliary compartment was filled with 35 mL phosphate buffer solution. After addition of complex **1**, cyclic voltammograms were recorded. After electrolysis, a 0.50 mL aliquot of the headspace was removed and replaced with 0.50 mL of CH_4. The headspace sample was injected into the gas chromatograph (GC). For the photocatalytic H_2 evolution, each sample was prepared in a 5 mL flask containing 4 mL of buffer in the presence of $[Ru(bpy)_3]Cl_2$, ascorbic acid, and complex **1**. The flask was sealed with a septum under air. Each sample was irradiated by LED light (469 nm) at room temperature under constant stirring. The amounts of H_2 produced during photocatalysis were determined by GC. GC experiments were carried out with an Agilent Technologies 7890A gas chromatography instrument. Spectrometer (EDS) measurement was carried out with a Shimadzu EPMA-1600 Electron Probe X-ray micro analyzer.

Synthesis of complex, $[L_2Co_2Cl_2]$ ***1:*** To a solution of H_2L (0.431 g, 1 mmol) and triethylamine (0.10 g, 1 mmol) in THF (20 ml), $CoCl_2 \cdot 6H_2O$ (0.238 g, 1 mmol) in methanol was added and the mixture was

stirred for 15 min. Single crystals were obtained from the filtrate which was allowed to stand at room temperature for several days, collected by filtration, and dried in *vacuo* (56%). The elemental analysis results (Found C, 43.37; H, 2.57; N, 5.12. $C_{20}H_{14}Cl_5N_2O_2Co$ requires C, 43.63; H, 2.56; N, 5.09) were in agreement with the formula of the sample used for X-ray analysis. IR bands (KBr pellets, cm^{-1}): 2858.86, 1605.43, 1459.28, 860.58, 751.39 (Fig. S20).

Crystal structure determination: The X-ray analysis of **1** was carried out with a Bruker SMART CCD area detector using graphite monochromated Mo-Kα radiation (λ = 0.71073 Å) at room temperature. All empirical absorption corrections were applied by using the SADABS program. [40] The structure was solved using direct methods and the corresponding non-hydrogen atoms are refined anisotropically. All the hydrogen atoms of the ligands were placed in calculated positions with fixed isotropic thermal parameters and included in the structure factor calculations in the final stage of full-matrix least-squares refinement. All calculations were performed using the SHELXTL computer program. [41] Crystallographic data for complex **1** were given in Table S1 and selected bond lengths and angles were listed in Tables S2-S3.

Conclusions

The cobalt(III) complex **1**, which is very easy to be obtained, can electrocatalyze and photocatalyze water reduction to generate H_2. Electrochemical studies show that **1** can electrocatalyze water reduction to hydrogen with a TOF of 789.6 moles of hydrogen per mole of catalyst per hour at an overpotential of 837.6 mV (pH 7.0). Complex **1** in pH 6.0 aqueous solution under air, together with $[Ru(bpy)_3]Cl_2$ and ascorbic acid as a sacrificial electron donor, in the presence of blue light (λ_{max} = 469 nm) produces hydrogen with a TON = 912 mol of H_2 (mol of cat)$^{-1}$. This discovery has established a new chemical paradigm for creating water reduction catalysts that is highly active in aqueous media.

Acknowledgements

This work was supported by the National Science Foundation of China (No. 20971045, 21271073), and the Student Research Program (SRP) of South China University of Technology.

Notes and references

College of Chemistry and Chemical Engineering, South China University of Technology, Guangzhou 510640, China. E-mail: shzhzhan@scut.edu.cn.

† Electronic Supplementary Information (ESI) available: CCDC 1062610 contains the supplementary crystallographic data for this paper can be obtained free of charge via http://www.ccdc.cam.ac.uk/conts/retrieving.html Experimental section and the synthesis of complexes in this paper are included in the supporting information. See DOI: 10.1039/c000000x/

1 T. J. Meyer, *Acc. Chem. Res*., 1989, **22**, 163-170.

2 J. A. Turner, *Science* 2004, **305**, 972-974.

3 H. B. Gray, *Nat. Chem*., 2009, **1**, 7-7.

4 R. Eisenberg and H. B. Gray, *Inorg. Chem*., 2008, **47**, 1697-1699.

5 J. Barber, *Chem. Soc. Rev*., 2009, **38**, 185-196.

6 H. I. Karunadasa, C. J. Chang and J. R. Long, *Nature* 2010, **464**, 1329-1333.

7 L. A. Berben and J. C. Peters, *Chem. Commun*., 2010, 398-400.

8 C. C. L. McCrory, C. Uyeda and J. C. Peters, *J. Am. Chem. Soc*., 2012, **134**, 3164-3170.

9 Y. Sun, J. P. Bigi, N. A. Piro, M. L. Tang, J. R. Long and C. J. Chang, *J. Am. Chem. Soc*., 2011, **133**, 9212-9215.

10 H. I. Karunadasa, E. Montalvo, Y. Sun, M. Majda, J. R. Long and C. J. Chang, *Science* 2012, **335**, 698-702;

11 V. S. Thoi, Y. Sun, J. R. Long and C. J. Chang, *Chem. Soc. Rev*., 2013, **42**, 2388-2400.

12 C. C. L. McCrory, C. Uyeda and J. C. Peters, *J. Am. Chem. Soc*., 2012, **134**, 3164-3170.

13 A. F. Heyduk and D. G. Nocera, *Science* 2001, 293, 1639-1641.

14 A. J. Esswein and D. G. Nocera, *Chem. Rev*., 2007, **107,** 4022-4047.

15 Z. Han, W. R. McNamara, M.-S. Eum, P. L. Holland and R. Eisenberg, *Angew. Chem. Int. Ed*., 2012, **51**, 1667 –1670.

16 H. Lv, W. Guo, K. Wu, Z. Chen, J. Bacsa, D. G. Musaev, Y. V. Geletii, S. M. Lauinger, T. Lian, and C. L. Hill, *J. Am. Chem. Soc*., 2014, **136**, 14015−14018.

17 L. L. Zhou, L, Z. Fu, L. Z. Tang, Y. X. Zhang and S. Z. Zhan, *Int. J. Hydrogen Energy* 2015, **40**, 5099-5105.

18 J. L. Dempsey, B. S. Brunschwig, J. R. Winkler and H. B. Gray, *Acc. Chem. Res*., 2009, **42**, 1995-2004.

19 P. Zhang, M. Wang, J. Dong, X. Li, F. Wang, L. Wu and L. Sun, *J. Phys. Chem. C*., 2010, **114**, 15868-15874.

20 C. F. Leung, S. M. Ng, C. C. Ko, W. L. Man, J. Wu, L. Chen and T. C. Lau, *Energy Environ. Sci*., 2012, **5**, 7903-7909.

21 M. Guttentag, A. Rodenberg, C. Bachmann, A. Senn, P. Hamm and R. Alberto, *Dalton Trans*., 2013, **42**, 334-337.

22 Y. Hou, B. L. Abrams, P. C. K. Vesborg, M. E. Bj¨orketun, K. Herbst, L. Bech, A. M. Setti, C. D. Damsgaard, T. Pedersen, O. Hansen, J. Rossmeisl, S. Dahl, J. K. Nørskov and I. Chorkendorff, *Nat. Mater*., 2011, **10**, 434-438.

23 A. J. Esswein and D. G. Nocera, *Chem. Rev*., 2007, **107**, 4022-4047.

24 Y. Sun, J. P. Bigi, N. A. Piro, M. L. Tang, J. R. Long and C. J. Chang, *J. Am. Chem. Soc*., 2011, **133**, 9212−9215.

25 Y. Sun, J. Sun, J. R. Long, P. Yang and C. J. Chang, *Chem. Sci*., 2013, **4**, 118−124.

26 J. P. Bigi, T. E. Hanna, W. H. Harman, A. Chang and C. J. Chang, *Chem. Commun*., 2010, **46**, 958−960.

27 A. E. King, Y. Surendranath, N. A. Piro, J. P. Bigi, J. R. Long and C. J. Chang, *Chem. Sci*., 2013, **4**, 1578−1587.

28 W. M. Singh, T. Baine, S. Kudo, S. Tian, X. A. N. Ma, H. Zhou, N. J. DeYonker, T. C. Pham, J. C. Bollinger, G. L. Baker, B. Yan, C. E. Webster and X. Zhao, *Angew. Chem. Int. Ed*., 2012, **51**, 5941-5944.

29 B. H. Solis, Y. Yu and S. Hammes-Schiffer, *Inorg. Chem*., 2013, **52**, 6994-4999.

30 U. J. Kilgore, J. A. S. Roberts, D. H. Pool, A. M. Appel, M. P. Stewart, M. R. DuBois, W. G. Dougherty, W. S. Kassel, R. M. Bullock and D. L. DuBois, *J. Am. Chem. Soc*., 2011, **133**, 5861–5872.

31 J. L. Fillol, Z. Codolà, I. Garcia-Bosch, L. Gómez, J. J. Pla and M. Costas, *Nature Chem*., 2011, **3**, 807-813.

32 X. Hu, B. S. Brunschwig and J. C. Peter, *J. Am. Chem. Soc*., 2007, **129**, 8988-8998.

33 L. Z. Fu, L. L. Zhou, L. Z. Tang, Y. X. Zhang and S. Z. Zhan, *J. Power Sources* 2015, **280**, 453-458.

34 L. L. Zhou, L. Z. Fu, L. Z. Tang, Y. X. Zhang and S. Z. Zhan, Int. J. Hydrogen Energy 2015, **40**, 5099-5105.

35 J.A.S. Roberts, U.J. Kilgore, D.H. Pool, A.M. Appel, M.P. Stewart, M.R. DuBois, W.G. Dougherty, W.S. Kassel, R.M. Bullock and D.L. DuBois, J. Am. Chem. Soc., 2011, **133**, 5861-5872.

36 J. T. Muckermann and E. Fujita, Chem. Commun., 2011, **47**, 12456-12458.

37 J. Xie, Q. Zhou, C. Li, W. Wang, Y. Hou, B. Zhang and X. Wang, Chem. Commun., 2014, **50**, 6520-6522.

38 L. Tong, R. Zong and R. P. Thummel, *J. Am. Chem. Soc*., 2014, **136**, 4881-4884.

39 A. M. Reckling, D. Martin, L. N. Dawe, A. Decken and C.M. Kozak, *J. Organomet. Chem.,* 2011, **696**, 787-794.

40 G. M. Sheldrick, SADABS, Program for Empirical Absorption Correction of Area Detector Data, University of Götingen, Götingen, Germany, 1996.

41 G. M. Sheldrick, SHELXS 97, Program for Crystal Structure Refinement, University of Götingen, Götingen, Germany, 1997.

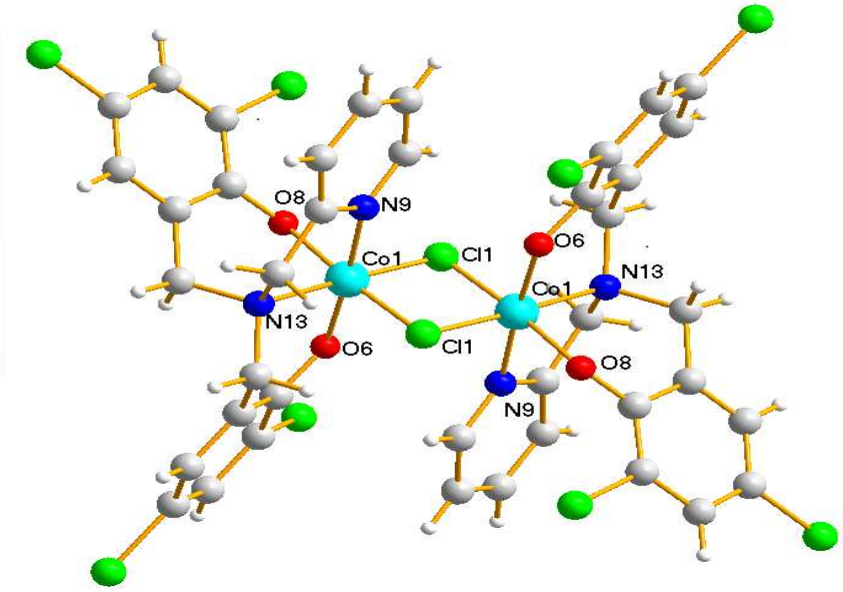

Fig. 1. Molecular structure of complex **1**.

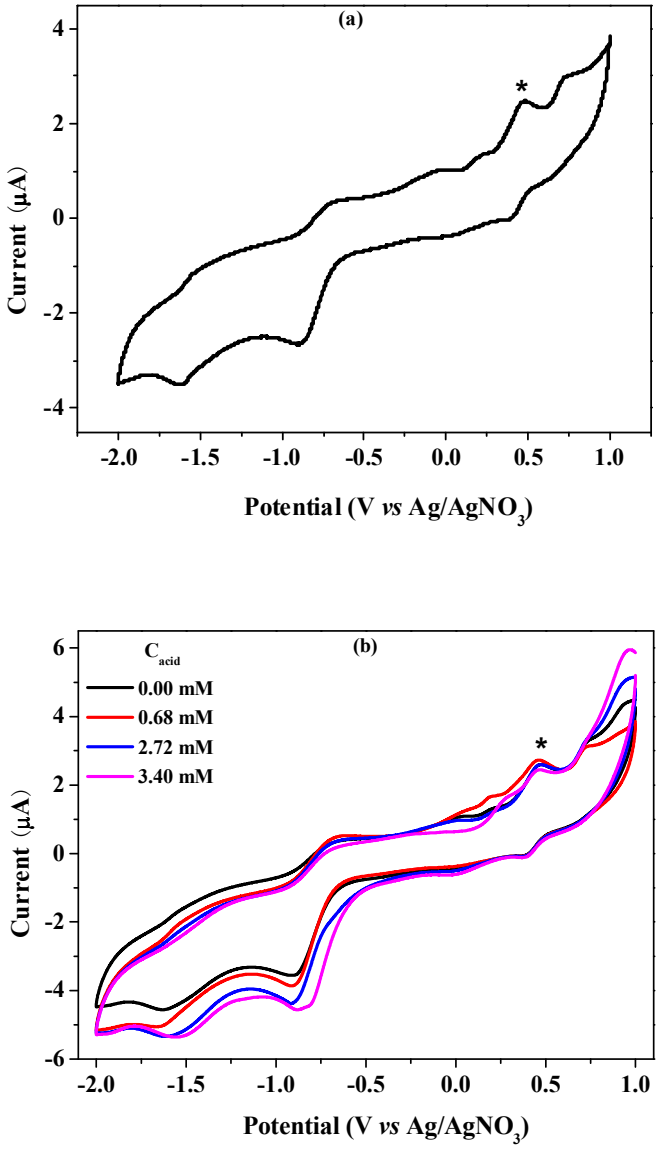

Fig. 2. (a) Cyclic voltammogram of 0.25 mM complex **1** in 0.10 M of [n-Bu_4N]ClO_4 DMF solution. (b) Cyclic voltammograms of a 0.25 mM solution of complex **1**, with varying concentrations of acetic acid in DMF. Conditions: 0.10 M [n-Bu_4N]ClO_4 as supporting electrolyte, scan rate: 100 mV/s, glassy carbon working electrode (1 mm diameter), Pt counter electrode, $Ag/AgNO_3$ reference electrode, Fc internal standard (*).

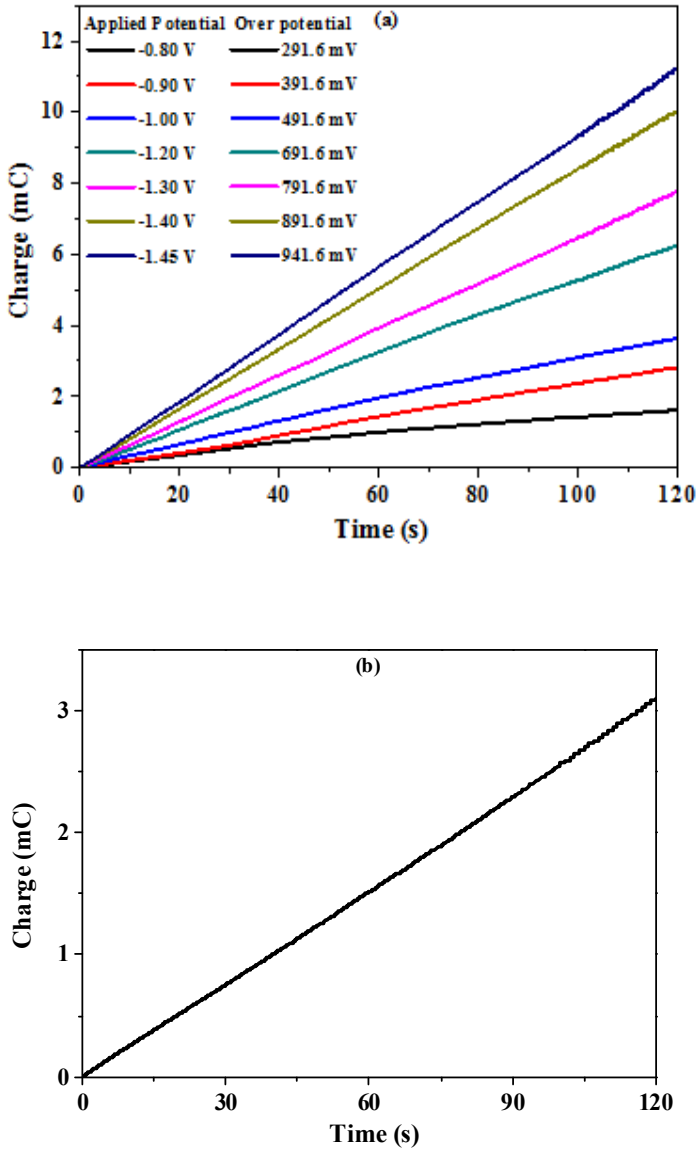

Fig. 3. (a) Charge buildup versus time from electrolysis of a 2.5 μM complex **1** in DMF (0.10 M [n-Bu_4N]ClO_4) under various applied potentials. All data have been deducted blank. (b) Charge buildup versus time from electrolysis of a 5.0 mM acetic acid in DMF (0.10 M [n-Bu_4N]ClO_4) under -1.45 V versus Ag/$AgNO_3$.

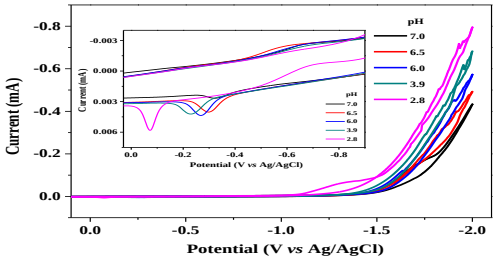

Fig. 4. CVs of 0.12 mM complex **1**, showing the variation in catalytic current with different pHs (scan rate: 100 mV/s). The inset shows a magnified view of the Co^{III}/Co^{II} couple.

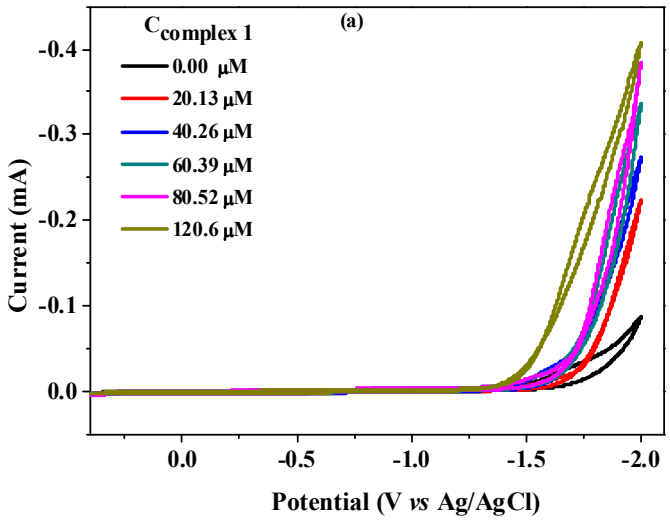
(a)
C complex 1
0.00 µM
20.13 µM
40.26 µM
60.39 µM
80.52 µM
120.6 µM
Current (mA)
-0.4
-0.3
-0.2
-0.1
0.0
0.0
-0.5
-1.0
-1.5
-2.0
Potential (V vs Ag/AgCl)

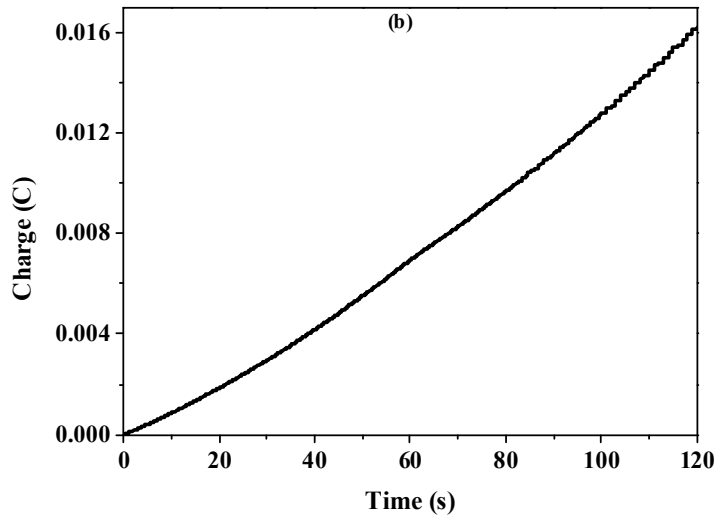
(b)
Charge (C)
0.016
0.012
0.008
0.004
0.000
0
20
40
60
80
100
120
Time (s)

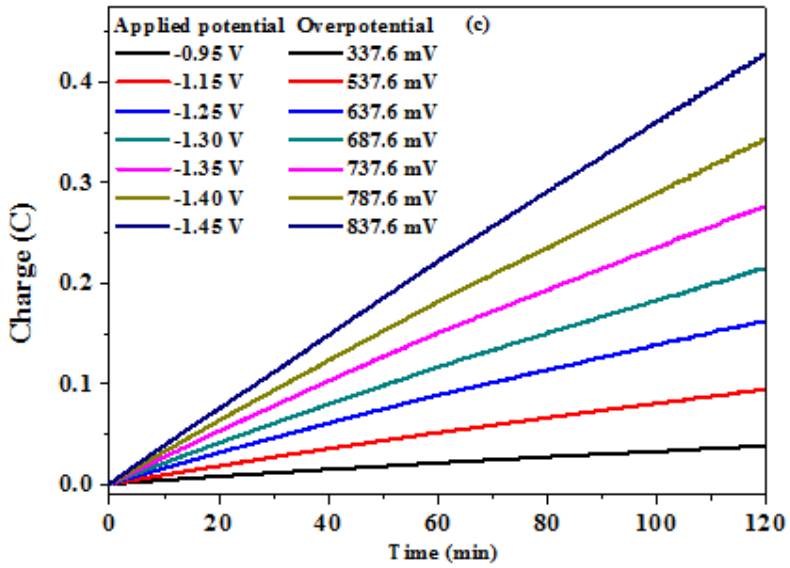

Fig. 5. (a) Cyclic voltammograms of complex **1** at various concentrations (pH 7.0, scan rate: 100 mV/s). (b) Charge buildup versus time from electrolysis of a 0.25 M buffer at pH 7.0. (c) Charge buildup versus time from electrolysis of complex **1** (2.0 μM) versus applied potentials at pH 7.0. All data have been deducted blank.

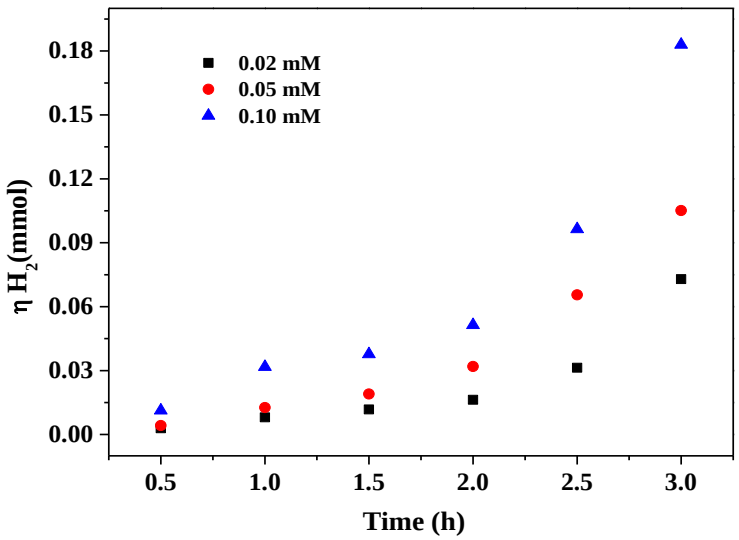

Fig. 6. Hydrogen evolution kinetics obtained upon continuous visible irradiation (λ = 469 nm) of pH 6.0 solutions (4 mL) containing 0.90 mM $Ru(bpy)_3Cl_2$, 0.15 M ascorbic acid, and **1** at 0.02 mM (black trace), 0.05 mM (red trace), and 0.10 mM (blue trace) concentration.